Received: 6 August 2018 | Revised: 2 January 2019 | Accepted: 9 February 2019

DOI: 10.1111/bcp.13902

ORIGINAL ARTICLE

# A semiphysiological population pharmacokinetic model of agomelatine and its metabolites in Chinese healthy volunteers

Feifan Xie[1] | An Vermeulen[1] | Pieter Colin[1,3] | Zeneng Cheng[2]

[1] Laboratory of Medical Biochemistry and Clinical Analysis, Faculty of Pharmaceutical Sciences, Ghent University, Ghent, Belgium

[2] Research Institute of Drug Metabolism and Pharmacokinetics, Xiangya School of Pharmaceutical Sciences, Central South University, Changsha, China

[3] Department of Anesthesiology, University of Groningen, University Medical Center Groningen, Groningen, The Netherlands

**Correspondence**
Feifan Xie, Laboratory of Medical Biochemistry and Clinical Analysis, Faculty of Pharmaceutical Sciences, Ghent University, Ottergemsesteenweg 460, B-9000 Ghent, Belgium.
Email: feifan.xie@ugent.be

**Aims:** Agomelatine is an antidepressant for major depressive disorders. It undergoes extensive first-pass hepatic metabolism and displays irregular absorption profiles and large interindividual variability (IIV) and interoccasion variability of pharmacokinetics. The objective of this study was to characterize the complex pharmacokinetics of agomelatine and its metabolites in healthy subjects.

**Methods:** Plasma concentration–time data of agomelatine and its metabolites were collected from a 4-period, cross-over bioequivalence study, in which 44 healthy subjects received 25 mg agomelatine tablets orally. Nonlinear mixed effects modelling was used to characterize the pharmacokinetics and variability of agomelatine and its metabolites. Deterministic simulations were carried out to investigate the influence of pathological changes due to liver disease on agomelatine pharmacokinetics.

**Results:** A semiphysiological pharmacokinetic model with parallel first-order absorption and a well-stirred liver compartment adequately described the data. The estimated IIV and interoccasion variability of the intrinsic clearance of agomelatine were 130.8% and 28.5%, respectively. The IIV of the intrinsic clearance turned out to be the main cause of the variability of area under the curve-based agomelatine exposure. Simulations demonstrated that a reduction in intrinsic clearance or liver blood flow, and an increase in free drug fraction had a rather modest influence on agomelatine exposures (range: −50 to 200%). Portosystemic shunting, however, substantially elevated agomelatine exposure by 12.6–109.1-fold.

**Conclusions:** A semiphysiological pharmacokinetic model incorporating first-pass hepatic extraction was developed for agomelatine and its main metabolites. The portosystemic shunting associated with liver disease might lead to significant alterations of agomelatine pharmacokinetics, and lead to substantially increased exposure.

KEYWORDS

agomelatine, first-pass, metabolite, pharmacokinetics, semiphysiological

The authors confirm that the PI for this paper is Zeneng Cheng and that he had direct clinical responsibility for patients.

  

## 1 | INTRODUCTION

**Agomelatine**, a **melatonin MT1** and **MT2** receptor agonist,[1,2] is a novel antidepressant for the treatment of major depressive disorders. It was approved for clinical use in Europe since 2009, where it is marketed under the names Valdoxan or Thymanax.[3] Agomelatine has a relatively favourable side effect profile, while providing similar therapeutic benefits compared to the antidepressants currently in use.[2,4] The recommended oral daily dose of agomelatine is 25 mg.

Agomelatine is classified as a biopharmaceutical classification system (BCS) class II drug with low solubility and high permeability.[5] Following oral administration, agomelatine is rapidly and almost completely (≥80%) absorbed, and it undergoes extensive hepatic first-pass metabolism.[5] Agomelatine is almost entirely metabolized by the hepatic cytochromes **CYP1A2** (90%) and **CYP2C9**/CYP2C19 (10%), with a very low urinary excretion of unchanged drug (0.01% of the dose).[5,6] The major metabolites, 3-hydroxy-agomelatine, 7-desmethyl-agomelatine, and 3-hydroxy-7-methoxy-agomelatine are not pharmacologically active and are rapidly conjugated and renally eliminated. The absolute oral bioavailability of this drug is approximately 1%, and its half-life is 1–2 hours. The interindividual variability (IIV) and interoccasion variability (IOV) in bioavailability is 160% and 104%, respectively, and is mainly driven by the first-pass effect and the interindividual differences in CYP1A2 activity.[5,6] The steady state volume of distribution of agomelatine is 35 L, while its plasma protein binding is 95% and does not depend on the concentration in the therapeutic range (5–1000 ng/ml).[5-7]

The pharmacokinetics (PK) of agomelatine have been studied in Caucasian and Chinese healthy volunteers and/or patients.[5,6,8,9] In a previous study on the bioequivalence of agomelatine formulations in Chinese male volunteers using reference-scaled average bioequivalence, no significant differences in relative bioavailability between the test and reference agomelatine formulations were found.[8] However, the atypical absorption profiles (i.e. the occurrence of double peaks and an apparent concentration plateau) and the origin of the huge variability were left uncharacterized. So far, there are no reports describing the population pharmacokinetics of agomelatine and its metabolites.

The present study aimed to characterize the pharmacokinetics of agomelatine and its metabolites and to quantify sources of variability using a mechanistic modelling approach. The study objectives were: (i) to develop a semiphysiological population PK model incorporating the first-pass effect for agomelatine and its metabolites; (ii) to describe the absorption process and identify the IIV and IOV of agomelatine; and (iii) to study the sensitivity of the different components of the semiphysiological model on agomelatine exposure.

### What is already known about this subject

- Agomelatine undergoes extensive first-pass hepatic metabolism and displays irregular absorption profiles and large interindividual variability and interoccasion variability of pharmacokinetics.
- Substantial alterations of agomelatine pharmacokinetics were reported in patients with hepatic impairment.
- The noncompartmental pharmacokinetics of agomelatine and its metabolites have been published. However, there has been no previous attempt to integrate the results into a (semiphysiological) population pharmacokinetic model for characterize the complex pharmacokinetics of agomelatine and its metabolites.

### What this study adds

- We show a detailed example of constructing a semiphysiological pharmacokinetic model through incorporating first-pass hepatic extraction to characterize the pharmacokinetics of agomelatine and its metabolites and to quantify sources of variability.
- Through deterministic simulations with this semiphysiological model, a substantially more-than-dose-proportional increase in agomelatine exposures in relation to portosystemic shunting in the presence of liver disease was observed.

## 2 | METHODS

### 2.1 | Study data

The data were obtained from a randomized sequence, 2-treatment and 4-period cross-over study of agomelatine administration to 44 healthy Chinese male subjects published previously.[8] Briefly, during the 4 treatment sessions separated by a 1-day washout period, the volunteers were orally administered 25 mg agomelatine reference formulation (Valdoxan™, Servier, France) or test formulation (Chongqing Fuke pharmaceutical group Co., Ltd., China). The baseline characteristics of study patients are summarized in Table 1. All subjects had normal hepatic and renal functions, and were nonsmokers. No drugs were taken for all subjects at least 2 weeks before the start of this study. The study protocol was approved by the institutional review board of Third Xiangya Hospital of Central South University (approval number: 12066).

**TABLE 1** Baseline characteristics of study patients ($n$ = 44)

| Characteristics | Median (interquartile range) |
|---|---|
| Age (y) | 22 (21–24) |
| Height (cm) | 171 (168–175) |
| Body weight (kg) | 60 (56–65) |
| Body mass index (kg/m$^2$) | 20.2 (19.4–21.6) |
| Serum creatinine (μmol/L) | 81.5 (74.8–88.0) |
| Alanine transaminase (U/L) | 16 (12–20) |
| Aspartate aminotransferase (U/L) | 19.5 (16.0–22.3) |
| Total bilirubin (μmol/L) | 13.4 (11.3–16.5) |

Venous blood samples were collected before the administration and at serial time points up to 8 hours postdose. Plasma was separated by centrifugation and stored at −40°C until analysis. The agomelatine, 3-hydroxy-agomelatine and 7-desmethyl-agomelatine concentrations were determined by a validated LC–MS/MS method.[10] The lower limit of quantification of agomelatine, 7-desmethyl-agomelatine and 3-hydroxy-agomelatine in plasma were 0.046, 0.137 and 0.460 ng/mL, respectively. The method precisions were <6.6% and accuracies were in the range of 90.2–105.1%.

A total of 2464 plasma samples were analysed for the simultaneous determination of agomelatine, 7-desmethyl-agomelatine, and 3-hydroxy-agomelatine. 408 (16.5%) of agomelatine concentrations were reported as below the limit of quantification (BLQ). 560 (22.7%) of 7-desmethyl-agomelatine samples were documented as BLQ, and 52 (2.1%) of 3-hydroxy-agomelatine measurements were regarded as BLQ.

## 2.2 | Model development and evaluation

Population PK modelling was performed in NONMEM (version 7.3, Icon Development Solutions, Ellicott City, MD, USA), assisted by Perl-Speaks-NONMEM (version 4.60, Uppsala University, Uppsala, Sweden) in combination with the Pirana software (version 2.9.6)[11] as graphical interface. The stochastic approximation expectation–maximization method was used to estimate parameters, combined with the importance sampling method assisted by mode a posteriori estimation (IMPMAP) to calculate the objective function for hypothesis testing. Beal's M3 method was used to handle BLQ data of agomelatine and 7-desmethyl-agomelatine.[12,13] The BLQ data of 3-hydroxy-agomelatine were dropped directly as it was only 2.1%. Data processing and graphical evaluation were carried out in R (version 3.4.1, R Foundation for Statistical Computing, Vienna, Austria).

Our model building started with a semiphysiological model accounting for the first-pass effect, previously proposed for other drugs with a high hepatic extraction ratio.[14,15] In short, a hepatic compartment is introduced to account for the conversion of agomelatine to its metabolites both pre-systemically and systemically. A well-stirred hepatic elimination is assumed taking into account hepatic blood flow ($Q_H$), agomelatine plasma protein binding ($f_u$) and intrinsic clearance ($CL_{int}$). The latter is comprised of 3 components, conversion of agomelatine to 7-desmethyl-agomelatine, agomelatine to 3-hydroxy-agomelatine, and agomelatine to other species. The formation of metabolites in the hepatic compartment was assumed to be first-order. The elimination of unchanged agomelatine by the kidney is negligible and was assumed to be 0.

**TABLE 2** Population pharmacokinetics model development procedure for agomelatine and its metabolites

| Mod no. | Ref no. | OFV (mean ± SD) | ΔOFV | AIC | Residual error variances (log-domain) | | | No. of parameters | Description |
|---|---|---|---|---|---|---|---|---|---|
| | | | | | Agomelatine | 3-hydroxy-agomelatine | 7-desmethyl-agomelatine | | |
| 1 | | 3299.7 ± 0.9 | | 3333.7 | 0.691 | 0.349 | 0.521 | 17 | First-order absorption + pre-systemic model + 1-compartment model for agomelatine and its metabolites |
| 4 | 1 | 1712.8 ± 2.8 | −1586.6 | 1762.8 | 0.536 | 0.248 | 0.382 | 25 | Parallel first-order absorption |
| 10 | 4 | −1423.1 ± 2.7 | −3135.9 | −1371.1 | 0.359 | 0.109 | 0.218 | 26 | Add IOV on $K_{13}$ |
| 18 | 10 | −3791.1 ± 8.8 | −2368.0 | −3737.1 | 0.309 | 0.082 | 0.190 | 27 | Add IOV on ALAG2 |
| 25 | 18 | −6035.9 ± 1.6 | −2244.8 | −5979.9 | 0.268 | 0.064 | 0.145 | 28 | Add IOV on $K_{23}$ |
| 26 | 25 | −6738.4 ± 2.0 | −702.5 | −6680.4 | 0.215 | 0.066 | 0.157 | 29 | Add IOV on $CL_{int}$ |
| 30 | 26 | −7763.9 ± 2.4 | −1025.5 | −7701.9 | 0.191 | 0.069 | 0.108 | 31 | Add peripheral compartment for 7-desmethyl-agomelatine, and fix IIV_$V_7$ due to estimated variance near to zero |
| 32 | 30 | −7943.6 ± 1.8 | −179.7 | −7879.6 | 0.182 | 0.051 | 0.088 | 32 | Add IOV on F1 |
| 34 | 32 | −8753.7 ± 2.5 | −810.1 | −8685.7 | 0.147 | 0.057 | 0.082 | 34 | Add peripheral compartment for agomelatine, and fix IIV_$Q_{7DM}$ and IIV_$V_8$ to 0 due to large relative standard error |
| 36 (final model) | 34 | −8684.4 ± 10.4 | 69.3 | −8616.4 | 0.152 | 0.052 | 0.089 | 34 | Add correlations for the formation fractions and clearances, respectively, between 7-desmethyl-agomelatine and 3-hydroxyagomelatine (this reduced model uncertainty) |

AIC, Akaike's information criterion; IIV, interindividual variability; IOV, interoccasion variability; OFV, objective function value.

Equations 1–3 describe the well-stirred model[16] and define the hepatic extraction ratio ($E_H$), hepatic plasma clearance ($CL_H$), and the fraction of absorbed drug escaping hepatic first-pass extraction ($F_H$)

$$E_H = f_{ub} \times CL_{int}/(Q_H + f_{ub} \times CL_{int}) \quad (1)$$

$$CL_H = Q_H \times E_H/PBR \quad (2)$$

$$F_H = 1 - E_H \quad (3)$$

In these equations, $f_{ub}$ is the ratio of unbound concentration in plasma to whole blood concentration, which is the mathematical product of unbound fraction of drug concentration in plasma ($f_u$) and plasma to blood drug concentration ratio (PBR). The $f_u$ and PBR of agomelatine are reported to be 0.05 and 1.45, respectively.[6]

The hepatic volume ($V_H$) in litres was associated to the subject body weight (WT, kg) as indicated by Noda et al.[17] in Equation 4:

$$V_H = 0.05012 \times WT^{0.78} \quad (4)$$

Hepatic blood flow in males was reported as 50.4 L/h/L of hepatic volume.[18]

$$Q_H = 50.4 \times V_H \quad (5)$$

To describe the disposition of agomelatine and its metabolites, both 1- and 2-compartmental models were tested. Regarding the absorption of agomelatine from the gut to the hepatic compartment, various absorption models with or without a lag time were tested, including single or parallel first-order absorption, single or parallel mixed 0- and first-order absorption, parallel transit compartment absorption, and single or parallel 0-order input into the depot and then first-order absorption.[19,20] Both linear and nonlinear (Michaelis–Menten) elimination of agomelatine from the hepatic compartment were tested.

The formation fractions of agomelatine to 3-hydroxy-agomelatine ($FM_{3OH}$) and of agomelatine to 7-desmethyl-agomelatine ($FM_{7DM}$) are described by Equations 6 and 7.

$$FM_{3OH} = \exp(\theta 3)/(1 + \exp(\theta 3) + \exp(\theta 4)) \quad (6)$$

$$FM_{7DM} = \exp(\theta 4)/(1 + \exp(\theta 3) + \exp(\theta 4)) \quad (7)$$

Where θ3 and θ4 are parameters describing the formation fractions. Additive normal distribution was assumed for the IIVs of θ3 and θ4.

When parallel absorption processes applied, a logit model was used for F1 representing the fraction of dose absorbed via gut depot

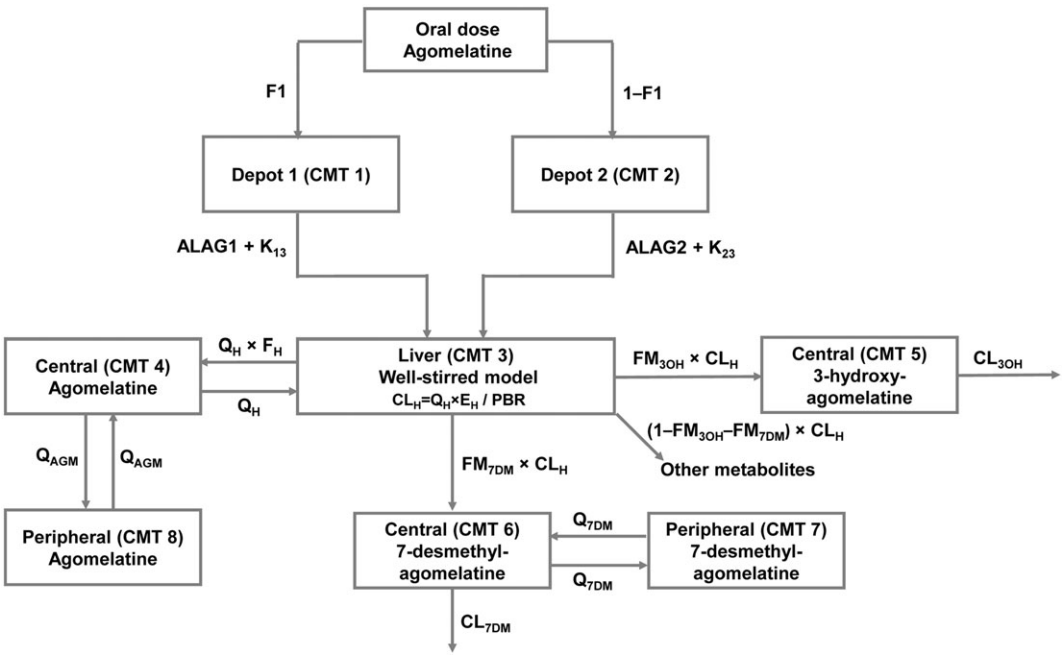


**FIGURE 1** Schematic representation of the semiphysiological pharmacokinetic model for agomelatine and its metabolites. F1, the fraction of dose absorbed via gut depot 1; $K_{13}$, first-order absorption rate constant through gut depot 1; $K_{23}$, first-order absorption rate constant through gut depot 2; ALAG1, absorption lag time of gut depot 1; ALAG2, absorption lag time of gut depot 2; $Q_H$, liver blood flow; $CL_H$, hepatic plasma clearance; $E_H$, hepatic extraction ratio; $F_H$, fraction of absorbed drug escaping hepatic first-pass; PBR, plasma to blood drug concentration ratio of agomelatine; $FM_{3OH}$, the fraction of agomelatine converted to 3-hydroxy-agomelatine; $FM_{7DM}$, the fraction of agomelatine converted to 7-desmethyl-agomelatine; $CL_{3OH}$, clearance of 3-hydroxy-agomelatine; $CL_{7DM}$, clearance of 7-desmethyl-agomelatine; $Q_{7DM}$, compartmental clearance between the central and peripheral compartment of 7-desmethyl-agomelatine; $Q_{AGM}$, compartmental clearance between the central and peripheral compartment of agomelatine

**TABLE 3** Parameter estimates of the pharmacokinetic model

| Parameter name | Estimate (RSE%)[a] [Shrinkage%] |
|---|---|
| Fixed effects (unit) | |
| $K_{13}$ (1/h) | 4.54 (19.0) |
| $V_4$ (L) | 64.6 (4.1) |
| $CL_{int}$ (L/h) | 111 000 (25.0) |
| $FM_{3OH}$ | exp(θ3)/(1 + exp(θ3) + exp(θ4)): 0.142 |
| $FM_{7DM}$ | exp(θ4)/(1 + exp(θ3) + exp(θ4)): 0.016 |
| θ3 | −1.78 (6.6) |
| θ4 | −3.95 (3.3) |
| $CL_{3OH}$ (L/h) | 44.9 (3.1) |
| $CL_{7DM}$ (L/h) | 52.9 (3.7) |
| ALAG1 (h) | 0.185 (4.0) |
| $K_{23}$ (1/h) | 4.23 (36.2) |
| ALAG2 (h) | 0.305 (30.7) |
| F1 | 0.681 (5.7) |
| $Q_{7DM}$ (L/h) | 28.1 (1.6) |
| $V_7$ (L) | 536 (1.4) |
| $Q_{AGM}$ (L/h) | 4.36 (26.1) |
| $V_8$ (L) | 157 (3.4) |
| Inter-individual variability (IIV) | |
| $K_{13}$ (CV%) | 32.6 (117.8)[21.9] |
| $V_4$ (CV%) | 19.5 (48.4)[0.1] |
| $CL_{int}$ (CV%) | 130.8 (32.5)[17.0] |
| θ3 (CV%) | 43.7 (88.0)[0.1] |
| θ4 (CV%) | 50.9 (41.3)[0.1] |
| $\omega_{\theta3,\theta4}$(covariance between θ3 and θ4) | 0.153 (75.8) |
| $CL_{3OH}$ (CV%) | 20.6 (14.7)[42.0] |
| $CL_{7DM}$ (CV%) | 28.4 (24.7)[38.5] |
| $\omega_{3OH,7DM}$ (covariance between $CL_{3OH}$ and $CL_{7DM}$) | 0.0492 (46.3) |
| ALAG1 (CV%) | 25.4 (11.4)[44.2] |
| $K_{23}$ (CV%) | 654.3 (12.3)[48.3] |
| ALAG2 (CV%) | 511.0 (8.4)[78.9] |
| F1[b] (CV%) | 83.2 (91.6)[27.9] |
| $Q_{7DM}$ (CV%) | 0 FIX |
| $V_7$ (CV%) | 0 FIX |
| $Q_{AGM}$ (CV%) | 181.8 (22.7)[20.7] |
| $V_8$ (CV%) | 0 FIX |
| Inter-occasional variability (IOV) | |
| $K_{13}$ (CV%) | 189.0 (8.4)[2.6–20.8] |
| ALAG2 (CV%) | 861.3 (2.9)[47.3–64.2] |
| $K_{23}$ (CV%) | 1220.2 (10.6)[0.1–29.4] |
| $CL_{int}$ (CV%) | 28.5 (37.0)[0.1–32.4] |
| F1 (CV%) | 302.9 (10.6)[15.8–35.6] |
| Residual variability | |
| Proportional error[c] (%) of agomelatine | 39.0 (8.5) [35.6] |

(Continues)

**TABLE 3** (Continued)

| Parameter name | Estimate (RSE%)[a] [Shrinkage%] |
|---|---|
| Proportional error[c] (%) of 3-hydroxy-agomelatine | 22.8 (8.3) [34.7] |
| Proportional error[c] (%) of 7-desmethyl-agomelatine | 29.7 (8.1) [24.5] |

ALAG1, absorption lag time of gut depot 1; ALAG2, absorption lag time of gut depot 2; $CL_{int}$, intrinsic clearance; $CL_{3OH}$, clearance of 3-hydroxy-agomelatine; $CL_{7DM}$, clearance of 7-desmethyl-agomelatine; F1, the fraction of dose absorbed via gut depot 1; $FM_{3OH}$, the fraction of agomelatine converted to 3-hydroxy-agomelatine; $FM_{7DM}$, the fraction of agomelatine converted to 7-desmethyl-agomelatine; $K_{13}$, first-order absorption rate constant through gut depot 1; $K_{23}$, first-order absorption rate constant through gut depot 2; $Q_{AGM}$, compartmental clearance between the central and peripheral compartment of agomelatine; $Q_{7DM}$, compartmental clearance between the central and peripheral compartment of 7-desmethyl-agomelatine; $V_4$ is the central volume of distribution of agomelatine; $V_7$, peripheral volume of distribution of 7-desmethyl-agomelatine; $V_8$, peripheral volume of distribution of agomelatine.

CV (%) is calculated according to: $CV\ (\%) = \sqrt{\exp(\omega^2) - 1} \times 100\%$. $\omega^2$: the variance estimate in the log-domain.

[a]RSE, relative standard error. RSEs were calculated from the $R^{-1}SR^{-1}$ matrix outputted by the $COVARIANCE step of NONMEM.

[b]Estimates of variability on F1 within the logit function.

[c]An additive error model in the log-transformed domain was used to characterize the residual unexplained variability, which approximates to a proportional error in the normal domain.

1. The additive random effect of F1 was used on the logit-scale. The individual values of F1 were thus constrained between 0 and 1 by using the inverse logit transformation on its random effect.

For all other parameters, IIV was assumed to be log-normally distributed. When applicable, IOV was taken into account. The residual error model was described by an additive error model using the log-transform-both-sides approach. The following covariates were tested: formulation (test *vs* reference), age, body weight, serum albumin, alanine transaminase and aspartate aminotransferase.

Model selection was guided by changes in the objective function value (OFV) between nested models, and Akaike's information criterion between non-nested models in combination with other metrics (e.g. % relative standard error of estimates, and residual error variance) and goodness of fit plots. For nested models, significance was assumed whenever the OFV decreased by >2× the standard deviation of the OFV during the IMPMAP evaluation.[21] The final model was validated by means of a visual predictive check (1000 simulations).

Extrapolation of the semiphysiological model from healthy adults to cirrhosis disease patients. Cirrhosis is frequently observed in the setting of alcoholic liver disease, and represents the final common pathway of a number of chronic liver diseases such as hepatitis B.[22] Cirrhosis may lead to portosystemic shunting, reduced plasma protein binding and decreased activity of drug-metabolizing enzymes (i.e. a reduction in $CL_{int}$), etc.[22,23] Portosystemic shunting may substantially decrease the presystemic elimination (i.e. first-pass effect) of high extraction drugs following their oral administration, thus resulting in a substantial increase in the bioavailability.[23] The influence of portosystemic shunting on hepatic extraction ratio was implemented as indicated below by the modification of Equation 1.[22,24]

$$E_H = f_{ub} \times CL_{int}/(Q_H + f_{ub} \times CL_{int}) \times (1 - f_{shunt}) \quad (8)$$

Where $f_{shunt}$ is the shunted fraction of total liver blood flow.

To investigate the effects of changes in the major determinants ($CL_{int}$, $f_u$, $Q_H$ and $f_{shunt}$) of hepatic drug clearance under liver disease, the final population PK model was used to conduct deterministic simulations to represent the typical population (mean) response. The simulation was performed with a single dose of 25 mg agomelatine given to patients weighing 70 kg under 4 scenarios: (i) 100% functional $CL_{int}$ under healthy conditions, and for decreases to 90, 80, 70, 60 and 50% of $CL_{int}$ under liver disease conditions; (ii) normal $f_u$ (0.05) under healthy conditions, increases to 1.2-, 1.4-, 1.6-, 1.8- and 2.0-fold of $f_u$; (iii) normal $Q_H$ for a healthy status, and reductions to 90, 80, 70, 60 and 50% of $Q_H$ under liver disease conditions; and (iv) no portosystemic shunting ($f_{shunt}$ is zero) for a healthy status, and $f_{shunt}$ increases to 10, 20, 30, 40 and 50% for liver disease conditions.

### 2.3 | Nomenclature of targets and ligands

Key protein targets and ligands in this article are hyperlinked to corresponding entries in http://www.guidetopharmacology.org, the common portal for data from the IUPHAR/BPS Guide to PHARMACOLOGY,[25] and are permanently archived in the Concise Guide to PHARMACOLOGY 2017/18.[26]

## 3 | RESULTS

### 3.1 | Model development and evaluation

The model development path is summarized in Table 2. The parallel first-order absorption model with an absorption lag time gave the lowest Akaike's information criterion among all of the tested absorption models and was thus selected for further model development. Adding IOVs in absorption-related parameters such as absorption lag time and absorption rate constants substantially improved the model fit (ΔOFV of −4612.8). IOV in $CL_{int}$ was significant, leading to a reduction of residual error variance of agomelatine from 0.268 to 0.215. Implementations of a peripheral compartment for 7-desmethyl-agomelatine, adding IOV on F1, and introducing a peripheral compartment for agomelatine further improved the model.

The final model comprised parallel first-order absorption from 2 gut depots to liver compartment, followed by 2-compartment model for agomelatine, 1-compartment model for 3-hydroxy-agomelatine, and 2-compartment model for 7-desmethyl-agomelatine. A schematic representation of the final model is depicted in Figure 1 and described in further detail below. The NONMEM code of final model is provided in the online supplement.

The rate of change of the amount of agomelatine in the liver compartment was described by Equation 9 as follows:

$$dA_H/dt = K_{13} \times A_1 + K_{23} \times A_2 - Q_H \times F_H \times A_H/V_H + Q_H \times A_4/V_4 - CL_H \times A_H/V_H \quad (9)$$

Where $A_1$, $A_2$, $A_H$, and $A_4$ are the amounts of agomelatine in the gut depot 1, depot 2, liver compartment, and central compartment, respectively. $K_{13}$ and $K_{23}$ are first-order absorption rate constants of depot 1 and depot 2, and $V_4$ is the central volume of distribution of agomelatine.

The rate of change of agomelatine, 3-hydroxy-agomelatine and 7-desmethyl-agomelatine in the central and peripheral compartments were described by Equation 10–14.

$$dA_4/dt = Q_H \times F_H \times A_H/V_H - Q_H \times A_4/V_4 - A_4 \times Q_{AGM}/V_4 + A_8 \times Q_{AGM}/V_8 \quad (10)$$

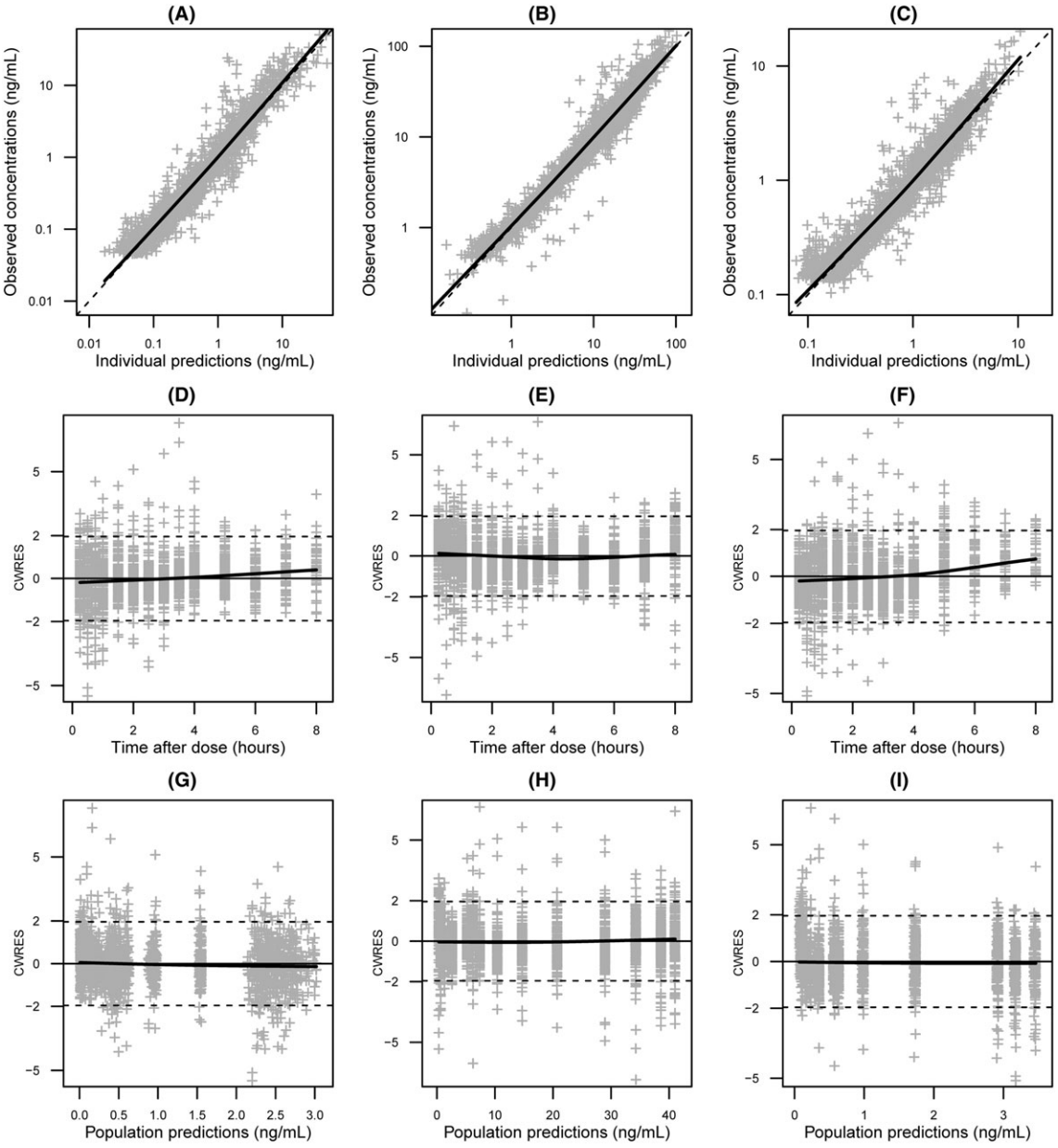


**FIGURE 2** Goodness-of-fit plots of the final population pharmacokinetics model for agomelatine and its metabolites. Top panels: observed concentrations *vs* individual predictions of agomelatine A, 3-hydroxy-agomelatine B, and 7-desmethyl-agomelatine C; Middle panels: conditional weighted residuals (CWRES) *vs* time after dose of agomelatine D, 3-hydroxy-agomelatine E, and 7-desmethyl-agomelatine F; Bottom panels: CWRES *vs* population predicted concentrations of agomelatine G, 3-hydroxy-agomelatine H, and 7-desmethyl-agomelatine I

$$dA_5/dt = FM_{3OH} \times CL_H \times A_H/V_H \times MPR1 - A_5 \times CL_{3OH}/V_5 \quad (11)$$

$$dA_6/dt = FM_{7DM} \times CL_H \times A_H/V_H \times MPR2 - A_6 \times CL_{7DM}/V_6 - A_6 \times Q_{7DM}/V_6 + A_7 \times Q_{7DM}/V_7 \quad (12)$$

$$dA_7/dt = A_6 \times Q_{7DM}/V_6 - A_7 \times Q_{7DM}/V_7 \quad (13)$$

$$dA_8/dt = A_4 \times Q_{AGM}/V_4 - A_8 \times Q_{AGM}/V_8 \quad (14)$$

Where $A_5$ is the amount of 3-hydroxy-agomelatine in central compartment, $A_6$ and $A_7$ are the amounts of 7-desmethyl-agomelatine in the central and peripheral compartment, and $A_8$ is the amount of agomelatine in the peripheral compartment. $CL_{3OH}$ and $CL_{7DM}$ are the clearances of 3-hydroxy-agomelatine and 7-desmethyl-agomelatine. $V_5$ and $V_6$ are the central volume of distributions of 3-hydroxy-agomelatine and 7-desmethyl-agomelatine, which were assumed to be equal to $V_4$ because of the identifiability issue. $V_7$ and $Q_{7DM}$ are the peripheral volume of distribution and compartmental clearance between the central and peripheral compartment for 7-desmethyl-agomelatine. $V_8$ and $Q_{AGM}$ are the peripheral volume of distribution and compartmental clearance between the central and peripheral compartment for agomelatine. MPR1 and MPR2 are molecular weight ratios of 3-hydroxy-agomelatine to agomelatine, and 7-desmethyl-agomelatine to agomelatine, accounting for the mass differences between agomelatine and its metabolites. MPR1 and MPR2 were 1.0658 and 0.9424, respectively.

None of the covariates, including formulation, was found to have a significant influence on the estimated PK parameters. Our results confirmed the previous bioequivalence finding using a noncompartmental analysis approach.[8] Population PK parameters of the final pharmacokinetic model are presented in Table 3. To evaluate the impact of the assumed $Q_H$ and $f_u$ on the final parameter estimates, a change to a 25% lower or higher $Q_H$ and $f_u$ was separately explored by sensitivity analysis, and percentage changes of the parameters were all within ±20%.

The goodness of fit plots demonstrate that the final model adequately described the data (Figure 2). Figure 3 shows the model's ability to describe the individual concentrations of agomelatine and its metabolites on different occasions for some selected representative patients. The individual predictions are in good agreement with the observations and are substantially different by each occasion and subject, reflecting the irregular and complex PK patterns of agomelatine and its metabolites. The visual predictive check plots indicate that the model generally captured the central tendency and spread of

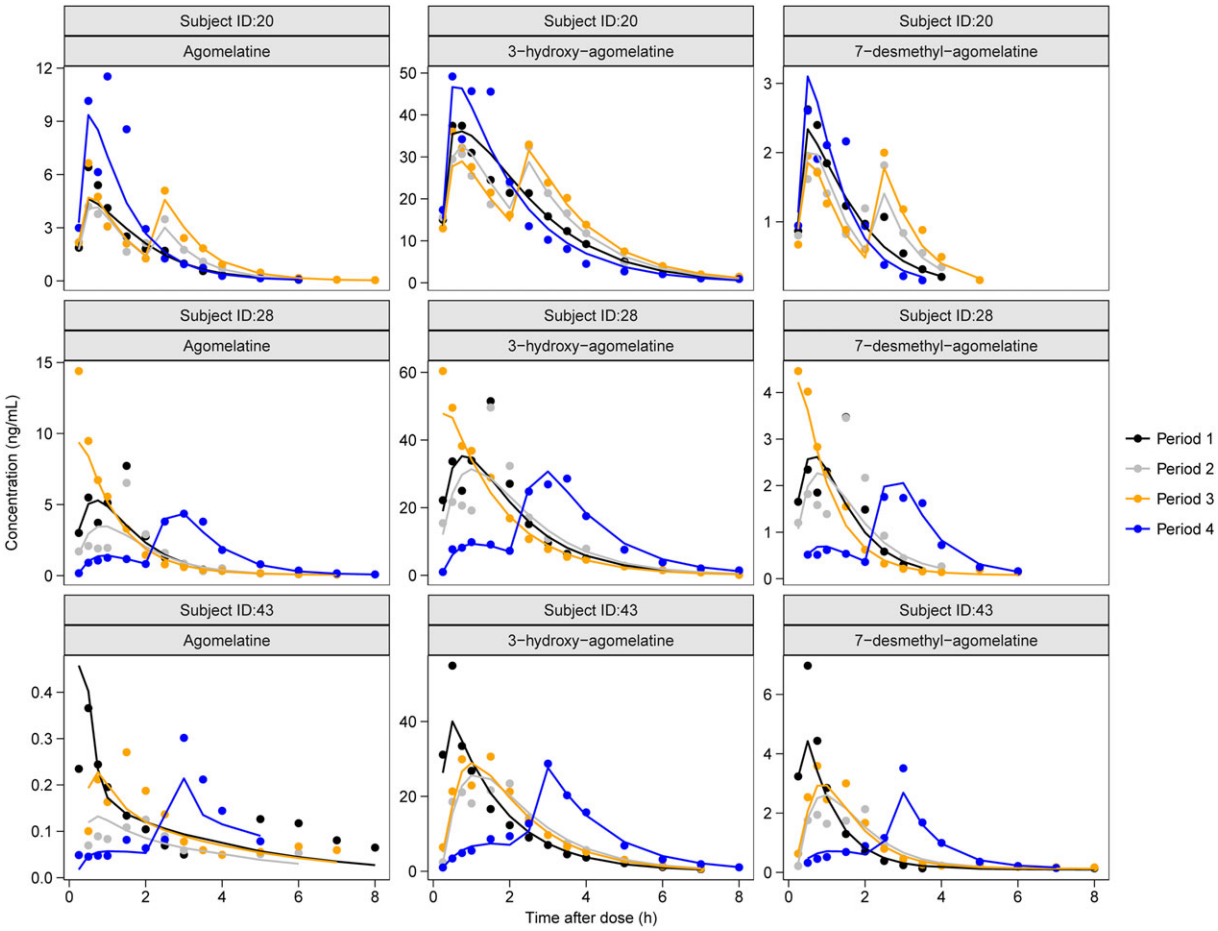


**FIGURE 3** Representative plasma concentrations and individual predictions of agomelatine and its metabolites on different occasions. The dots are observed concentrations, and the solid lines are individual predictions

observed plasma concentrations for agomelatine and its metabolites (Figure 4). Of the observations of agomelatine, 9.3% laid outside the 90% prediction interval. 6.1% and 6.8% of the observations of 3-hydroxy-agomelatine and 7-desmethyl-agomelatine fell outside the 90% prediction interval.

### 3.2 | Simulation-based analysis

The typical plasma concentration time-courses of agomelatine under healthy status and liver disease are shown in Figure 5. A 50% reduction of $CL_{int}$ leads to a doubling of agomelatine's maximum concentration ($C_{max}$) and area under the plasma concentration–time curve (AUC), while a 2-fold increase in $f_u$ results in a 50% decrease in $C_{max}$ and AUC. A 50% decrease in $Q_H$ causes a 40.8% lower agomelatine $C_{max}$ but unchanged AUC. Ten percent of portosystemic shunting leads to an increase of agomelatine $C_{max}$ and AUC by a factor of 12.6 and 13.9 respectively, and the values rise to 58.6 and 109.1 in case of 50% portosystemic shunting. Changes in $CL_{int}$ and $f_u$ do not significantly impact the half-life of agomelatine, while a 50% decline of $Q_H$ or the presence of 50% $f_{shunt}$ doubles the half-life of agomelatine. The simulations demonstrate that changes in $CL_{int}$, $f_u$ and $Q_H$ have minor impacts on agomelatine exposures. Instead, the presence of portosystemic shunting greatly increases the exposures of agomelatine. Both the reduction of $Q_H$ and the presence of portosystemic shunting significantly prolonged the half-life of agomelatine.

## 4 | DISCUSSION

An integrated population PK model of agomelatine and its metabolites incorporating parallel first-order absorption and hepatic first-pass extraction was developed in healthy subjects and the influence of pathological changes in liver disease on agomelatine's PK profile was investigated through a simulation approach.

Drugs with very low aqueous solubility are believed to exhibit dissolution-rate limited absorption thus atypical absorption profiles.[27,28] Agomelatine is slightly soluble in aqueous solution (<0.1 mg/ml) over the physiological pH range. In this study, secondary peaks (23 occasions, 12%), notable delayed absorptions (20 occasions, 10.4%), and the occurrence of a concentration plateau during the absorption phase (25 occasions, 13%) in the concentration–time profiles of agomelatine were observed following oral administration of agomelatine tablets to fasted subjects. These irregular PK phenomena cannot be well described by a conventional single-order absorption model. In our model, the parallel 1$^{st}$first-order absorption model with a lag time was applied representing different absorption rates and

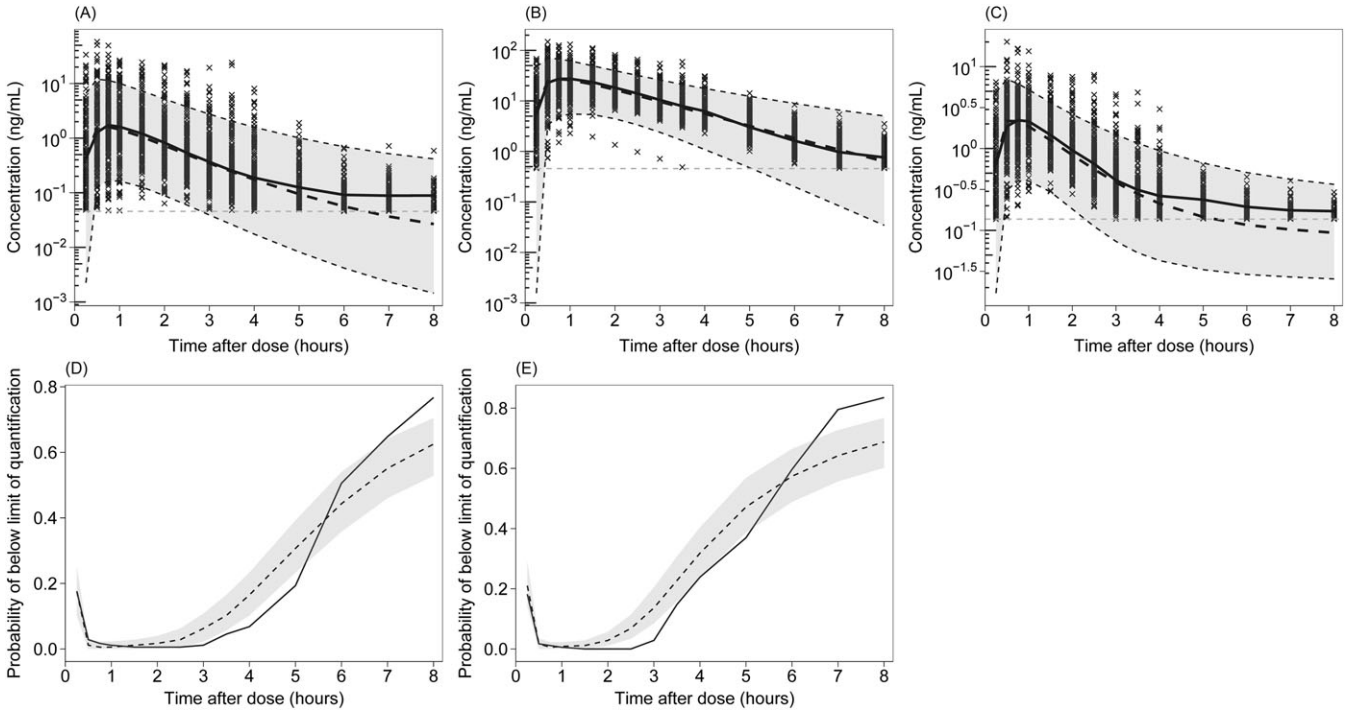


**FIGURE 4** Visual predictive check plots for the final population pharmacokinetics model of agomelatine A, and D, 3-hydroxy-agomelatine B, and 7-desmethyl-agomelatine C, and E. The upper panels represent simulation-based 90% prediction intervals (grey shaded areas) of the continuous data. The black solid line represents the median of the observations, and the black dashed line represents the median of the model predictions. The horizontal dashed lines indicate the lower limit of quantification (LLOQ) of agomelatine (0.046 ng/mL), 3-hydroxy-agomelatine (0.460 ng/mL), and 7-desmethyl-agomelatine (0.137 ng/mL). The lower panels display simulation based 90% confidence intervals (grey shaded areas) around the median (dashed black lines) for the fraction of below LLOQ observations. The observed fraction samples below LLOQ are represented with solid black lines

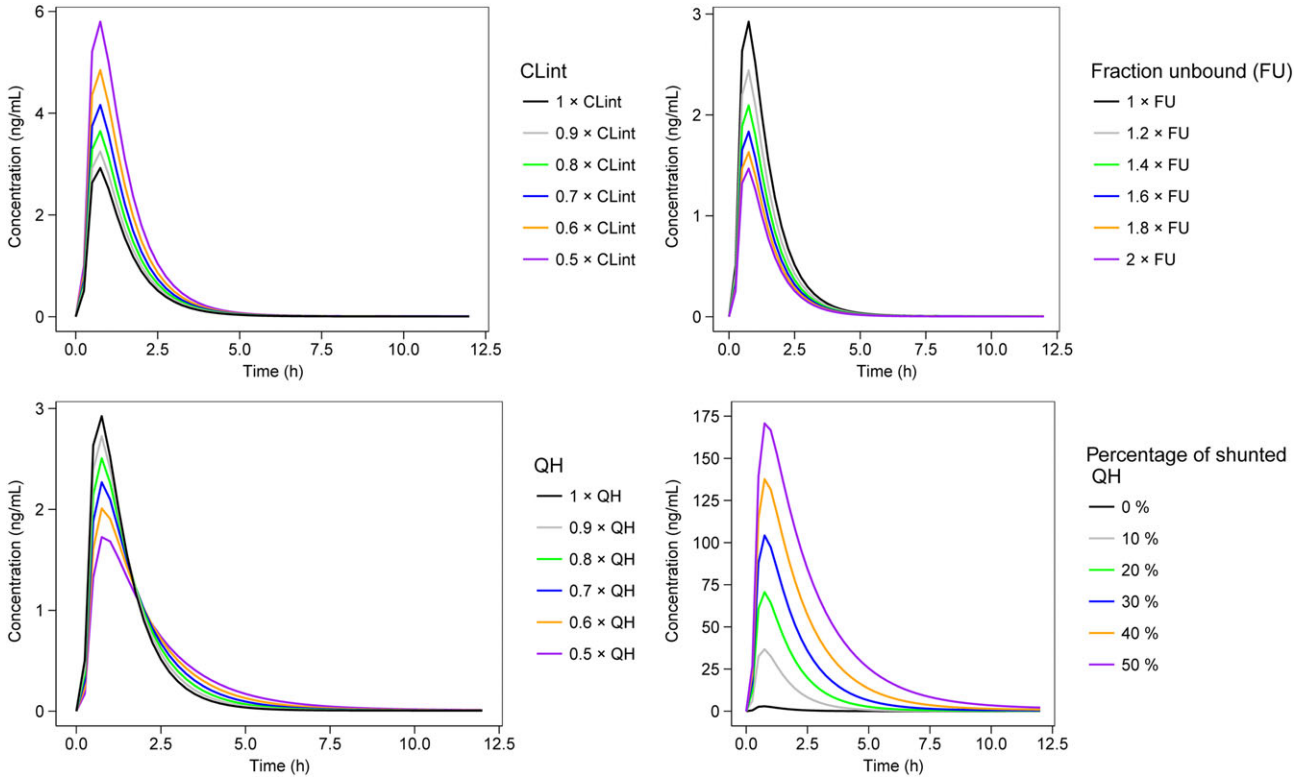


**FIGURE 5** Typical concentration–time profiles of agomelatine for healthy status and for liver disease. Top left panel: the impact of reductions in intrinsic clearance ($CL_{int}$) on agomelatine pharmacokinetics profile. Top right panel: the impact of increases in free plasma agomelatine fraction ($f_u$) on agomelatine pharmacokinetics profile. Bottom left panel: the impact of decreases in hepatic blood flow ($Q_H$) on agomelatine pharmacokinetics profile. Bottom right panel: the impact of extents of shunted fraction ($f_{shunt}$) of hepatic blood flow on agomelatine pharmacokinetics profile

lag times of agomelatine due to its different between-subject and between occasion dissolution rates and lag times in the gut sites.

Due to the extensive hepatic first-pass extraction of agomelatine following oral administration, the concentrations of metabolites are much higher than those of the parent drug agomelatine. To mechanistically integrate the PK profiles of agomelatine and its metabolites, we implemented a hepatic compartment describing the well-stirred model based hepatic extraction for agomelatine. According to the well-stirred model, the typical hepatic extraction ratio of agomelatine was 99.1%. Assuming that 80% of the dose is absorbed from the gut to the liver, the resulting bioavailability of agomelatine is 0.7%. The apparent volume of distribution was 64.6 L, and the apparent total clearance of agomelatine was 47.5 L/h. With the assumption of 80% dose absorption, the estimated systemic clearance of agomelatine would be 38 L/h in Chinese subjects. The clearance of agomelatine in Chinese subjects is lower than the corresponding value (66 L/h) in Caucasians.[5,6] This might be explained by the lower intrinsic clearance of CYP1A2 in Chinese population compared to Caucasians, as reported previously.[29]

The PK model demonstrated very large IOV and also IIV ($k_{23}$ and ALAG2) of absorption related parameters. This indicates that the absorption patterns greatly differ within subjects for each occasion and also between subjects, which reflects the irregular absorption phenomena of agomelatine. This could be the result from the environmental differences in the gut between subjects and the dynamically changing gut environment within subjects for the dissolution of agomelatine. Previous reports[6] declared that the interindividual differences of $CL_{int}$ are 1 of the sources leading to large variability of agomelatine exposures. Our study quantified the IIV and IOV of $CL_{int}$ as 130.8% and 28.5%, respectively. Given that the drug is at least 80% absorbed, our results indicate that the IIV of $CL_{int}$ is the main source for the variability of the AUC-based exposure of agomelatine.

Agomelatine is contraindicated in patients with hepatic impairment, as indicated in the drug insert package. It was shown that following oral administration of 25 mg agomelatine, the $C_{max}$ increased by a factor of 60 and 110, while AUC increased by 70 and 140 times, in cirrhotic patients with mild (Child–Pugh type A) and moderate (Child–Pugh type B) hepatic impairment, respectively, compared to healthy subjects.[6] Therefore, it is recommended to perform liver function tests in all patients receiving agomelatine at treatment initiation and during treatment. In this study, we used the developed model to further explore impacts of hepatic impairment to check the recommendations and as a further external validation of the semiphysiological model. Our simulations demonstrated that single alterations of $CL_{int}$, $f_u$, and $Q_H$ within 2-fold caused by the pathological changes in liver disease will not result in clinically relevant changes in drug exposures due to the high inter-individual variability of agomelatine pharmacokinetics, while the presence of portosystemic shunting is the most influential factor that significantly increases agomelatine exposures. Previous studies reported that a significant

degree (27%) to extensive shunting (70%) of live blood flow can occur in chronic liver disease patients.[30] Our simulation results of portosystemic shunting confirmed this many-fold observed increases in agomelatine exposures, and indicate that portosystemic shunting is the main underlying mechanism for the extreme increases in agomelatine exposures. It should be noted that our simulations only investigated the impact of single changes in each of the determinants of hepatic clearance. Clinically, the changes in hepatic blood flow, liver enzyme activity, plasma protein binding, and the presence of portosystemic shunting can occur alone and most often in combination.[23] When they coexist, their effect on drug PK is synergistic. Through the semiphysiological PK model, pharmacokinetic outcomes of these complicated situations that were not studied here can also be easily predicted.

One limitation of this study is that the (individual) metabolic capacity of liver CYP1A2 in the target population was not described in the model. CYP1A2 phenotyping (e.g. caffeine-based measurement of CYP1A2 activity)[31] was not carried out due to the bioequivalence study nature of the original study. Although the estimated $CL_{int}$ in the model can approximately represent the metabolic capacity of CYP1A2 since CYP1A2 accounts for 90% metabolism of agomelatine, it is a merit to further incorporate phenotyping based CYP1A2 activity into the model. An integrated semiphysiological model with CYP1A2 phenotyping would well predict metabolism extent of agomelatine beforehand, thus potentially useful for individualized dosing.

In conclusion, we have presented here for the first time a semiphysiological PK model including hepatic first-pass extraction for agomelatine and its main metabolites in healthy subjects. The proposed model adequately described the plasma concentration–time data of agomelatine and its metabolites. The model was used to simulate pharmacokinetic alterations in the presence of liver disease, and a substantially more-than-dose-proportional increase in agomelatine exposures in relation to portosystemic shunting was observed.

## COMPETING INTERESTS

A.V. is an 80% employee of Johnson and Johnson and owns J&J stock/stock options. She is also a visiting Professor at Ghent University. The other authors have no competing interests to declare.

## ACKNOWLEDGEMENTS

F.X. acknowledges the China Scholarship Council (CSC) for his Ph.D. grant.

## CONTRIBUTORS

Z.C. designed and implemented of the research. F.X. conceived of the presented idea and analysed the data with the input from A.V. and P.C. F.X. wrote the paper. A.V. and P.C. revised the manuscript.

## ORCID

*Feifan Xie* https://orcid.org/0000-0001-8427-4030
*Pieter Colin* https://orcid.org/0000-0003-3616-5539
*Zeneng Cheng* https://orcid.org/0000-0001-9352-9744

## REFERENCES

1. Srinivasan V, Cardinali DP, Pandi-Perumal SR, Brown GM. Melatonin agonists for treatment of sleep and depressive disorders. *J Exp Integr Med*. 2011;1(3):149-158.
2. MacIsaac SE, Carvalho AF, Cha DS, Mansur RB, McIntyre RS. The mechanism, efficacy, and tolerability profile of agomelatine. *Expert Opin Pharmacother*. 2014;15(2):259-274.
3. Sansone RA, Sansone LA. Agomelatine: a novel antidepressant. *Innov Clin Neurosci*. 2011;8:10.
4. Eser D, Baghai TC, Möller H-J. Agomelatine: the evidence for its place in the treatment of depression. *Core Evid*. 2009;4:171.
5. TGA.Gov.au. Australian Public Assessment Report for Agomelatine, 2010. https://www.tga.gov.au/sites/default/files/auspar-valdoxan.pdf. Accessed August 6, 2018.
6. EMA.Europa.eu. CHMP ASSESSMENT REPORT FOR Valdoxan, 2008. http://www.ema.europa.eu/docs/en_GB/document_library/EPAR_-_Public_assessment_report/human/000915/WC500046226.pdf. Accessed August 6, 2018.
7. Howland RH. Critical appraisal and update on the clinical utility of agomelatine, a melatonergic agonist, for the treatment of major depressive disease in adults. *Neuropsychiatr Dis Treat*. 2009;5:563.
8. Tang F, Zhou R, Cheng Z, et al. Implementation of a reference-scaled average bioequivalence approach for highly variable generic drug products of agomelatine in Chinese subjects. *Acta Pharm Sin B*. 2016;6(1):71-78.
9. Li C, Xu J, Zheng Y, et al. Bioequivalence and pharmacokinetic profiles of agomelatine 25-mg tablets in healthy Chinese subjects: a four-way replicate crossover study demonstrating high intra-and inter-individual variations. *Chem Pharm Bull*. 2017;65(6):524-529.
10. Li M, Tang F, Xie F, et al. Development and validation a LC–MS/MS method for the simultaneous determination of agomelatine and its metabolites, 7-desmethyl-agomelatine and 3-hydroxy-agomelatine in human plasma: Application to a bioequivalence study. *J Chromatogr B Analyt Technol Biomed Life Sci*. 2015;1003:60-66.
11. Keizer RJ, Karlsson M, Hooker A. Modeling and simulation workbench for NONMEM: tutorial on Pirana, PsN, and Xpose. *CPT Pharmacomet Syst Pharmacol*. 2013;2:1-9.
12. Beal SL. Ways to fit a PK model with some data below the quantification limit. *J Pharmacokinet Pharmacodyn*. 2001;28(5):481-504.
13. Ahn JE, Karlsson MO, Dunne A, Ludden TM. Likelihood based approaches to handling data below the quantification limit using NONMEM VI. *J Pharmacokinet Pharmacodyn*. 2008;35(4):401-421.
14. Gordi T, Xie R, Huong NV, Huong DX, Karlsson MO, Ashton M. A semiphysiological pharmacokinetic model for artemisinin in healthy subjects incorporating autoinduction of metabolism and saturable first-pass hepatic extraction. *Br J Clin Pharmacol*. 2005;59(2):189-198.
15. Chirehwa MT, Rustomjee R, Mthiyane T, et al. Model-based evaluation of higher doses of rifampin using a semimechanistic model incorporating autoinduction and saturation of hepatic extraction. *Antimicrob Agents Chemother*. 2016;60(1):487-494.
16. Rowland M, Tozer TN, Derendorf H, Hochhaus G. *Clinical pharmacokinetics and pharmacodynamics: concepts and applications*. Philadelphia, PA: Wolters Kluwer Health/Lippincott William & Wilkins; 2011.
17. Noda T, Todani T, Watanabe Y, Yamamoto S. Liver volume in children measured by computed tomography. *Pediatr Radiol*. 1997;27(3):250-252.
18. Rabbie SC, Martin PD, Flanagan T, Basit AW, Standing JF. Estimating the variability in fraction absorbed as a paradigm for informing

formulation development in early clinical drug development. *Eur J Pharm Sci*. 2016;89:50-60.

19. Pétricoul O, Cosson V, Fuseau E, Marchand M. Population models for drug absorption and enterohepatic recycling. In: Ette EI, Williams PJ, eds. *Pharmacometrics: the science of quantitative pharmacology*. Hoboken, NJ: John Wiley & Sons, Inc; 2007:345-382.
20. Owen JS, Fiedler-Kelly J. *Introduction to population pharmacokinetic/pharmacodynamic analysis with nonlinear mixed effects models*. Hoboken, NJ: John Wiley & Sons; 2014.
21. Hard ML, Mills RJ, Sadler BM, Turncliff RZ, Citrome L. Aripiprazole lauroxil: pharmacokinetic profile of this long-acting injectable antipsychotic in persons with schizophrenia. *J Clin Psychopharmacol*. 2017;37(3):289-295.
22. Susla GM, Lertora JJ. Effect of liver disease on pharmacokinetics. In: *Principles of Clinical Pharmacology*. Third ed. Amsterdam: Elsevier; 2013:81-96.
23. Verbeeck RK. Pharmacokinetics and dosage adjustment in patients with hepatic dysfunction. *Eur J Clin Pharmacol*. 2008;64(12):1147-1161.
24. McLean A, Souich P, Gibaldi M. Noninvasive kinetic approach to the estimation of total hepatic blood flow and shunting in chronic liver disease—a hypothesis. *Clin Pharmacol Ther*. 1979;25(2):161-166.
25. Harding SD, Sharman JL, Faccenda E, et al. The IUPHAR/BPS Guide to PHARMACOLOGY in 2018: updates and expansion to encompass the new guide to IMMUNOPHARMACOLOGY. *Nucl Acids Res*. 2017;46:D1091-D1106.
26. Alexander SP, Fabbro D, Kelly E, et al. The concise guide to PHARMACOLOGY 2017/18: enzymes. *Br J Pharmacol*. 2017;174:S272-S359.
27. Wong S, Kellaway I, Murdan S. Enhancement of the dissolution rate and oral absorption of a poorly water soluble drug by formation of surfactant-containing microparticles. *Int J Pharm*. 2006;317(1):61-68.
28. Martinez MN, Amidon GL. A mechanistic approach to understanding the factors affecting drug absorption: a review of fundamentals. *J Clin Pharmacol*. 2002;42(6):620-643.
29. Yang J, He MM, Niu W, et al. Metabolic capabilities of cytochrome P450 enzymes in Chinese liver microsomes compared with those in Caucasian liver microsomes. *Br J Clin Pharmacol*. 2012;73(2):268-284.
30. Williams RL, Mamelok RD. Hepatic disease and drug pharmacokinetics. *Clin Pharmacokinet*. 1980;5(6):528-547.
31. Faber MS, Jetter A, Fuhr U. Assessment of CYP1A2 activity in clinical practice: why, how, and when? *Basic Clin Pharmacol Toxicol*. 2005;97(3):125-134.

## SUPPORTING INFORMATION

Additional supporting information may be found online in the Supporting Information section at the end of the article.

**How to cite this article:** Xie F, Vermeulen A, Colin P, Cheng Z. A semiphysiological population pharmacokinetic model of agomelatine and its metabolites in Chinese healthy volunteers. *Br J Clin Pharmacol*. 2019;85:1003–1014. https://doi.org/10.1111/bcp.13902